electronics

MDPI

Article

Information Fusion for 5G IoT: An Improved 3D Localisation Approach Using K-DNN and Multi-Layered Hybrid Radiomap

Brahim El Boudani [1,*], Tasos Dagiuklas [1], Loizos Kanaris [2], Muddesar Iqbal [1] and Christos Chrysoulas [3]

[1] School of Engineering, London South Bank University, London SE1 0AA, UK; tdagiuklas@lsbu.ac.uk (T.D.); m.iqbal@lsbu.ac.uk (M.I.)
[2] Signit Solutions Ltd., Nicosia 2311, Cyprus; l.kanaris@sigintsolutions.com
[3] School of Computing, Edinburgh Napier University, Edinburgh EH11 4BN, UK; c.chrysoulas@napier.ac.uk
* Correspondence: elboudab@lsbu.ac.uk; Tel.: +44-20-7815-7815

Abstract: Indoor positioning is a core enabler for various 5G identity and context-aware applications requiring precise and real-time simultaneous localisation and mapping (SLAM). In this work, we propose a K-nearest neighbours and deep neural network (K-DNN) algorithm to improve 3D indoor positioning. Our implementation uses a novel data-augmentation concept for the received signal strength (RSS)-based fingerprint technique to produce a 3D fused hybrid. In the offline phase, a machine learning (ML) approach is used to train a model on a radiomap dataset that is collected during the offline phase. The proposed algorithm is implemented on the constructed hybrid multi-layered radiomap to improve the 3D localisation accuracy. In our implementation, the proposed approach is based on the fusion of the prominent 5G IoT signals of Bluetooth Low Energy (BLE) and the ubiquitous WLAN. As a result, we achieved a 91% classification accuracy in 1D and a submeter accuracy in 2D.

Keywords: indoor localisation; 5G IoT; deep learning; machine learning; information fusion; tracking; Internet of Things

Citation: El Boudani, B.; Dagiuklas, T.; Kanaris, L.; Iqbal, M.; Chrysoulas, C. Information Fusion for 5G IoT: An Improved 3D Localisation Approach Using K-DNN and Multi-Layered Hybrid Radiomap. *Electronics* **2023**, *12*, 4150. https://doi.org/10.3390/electronics12194150

Academic Editor: Franco Cicirelli

Received: 27 August 2023
Revised: 25 September 2023
Accepted: 29 September 2023
Published: 5 October 2023

1. Introduction

Supported by AI (artificial intelligence) and IoT (Internet of Things), 3D positioning is a core enabler for various 5G identity and context-aware applications requiring precise and real-time simultaneous localisation and mapping (SLAM) both indoors and outdoors [1]. Typical scenarios include mobile robots (MRs) performing surgery on a patient, autonomous ground vehicles (AGVs) docking newly arrived products in a smart factory, and unmanned aerial vehicles (UAVs) monitoring crops' status [2–4]. Very recently, a Cisco report [5] predicted an increase in the number of these specialised IoT devices connected to the internet from 8.8 billion in 2018 to 13.1 billion by 2023—1.4 billion of them will be 5G-capable. In this respect, while space giants (SpaceX and Lockheed Martin) [6] are working to improve the outdoor accuracy of GPS III to below 3 m, heterogeneous 5G IoT networks (HetNets) represent themselves as an indispensable source for improving indoor positioning systems (IPSs).

A 3rd Generation Partnership Project (3GPP) release established the requirements for improved indoor/outdoor 3D localisation using a RAT-independent positioning scheme for vertical and horizontal sectors [7]. Therefore, this specification put a strong emphasis on seamless collaborations and fusion between various radio technologies, such as device-to-device communication, ultra-dense communication, millimetre wave (mm wave), sub-6 GHz, and vehicle-to-everything (V2X) [8], and protocols such as IEEE 802.15.1 (Bluetooth Low Energy), IEEE 802.11be (extremely High Throughput WLAN), and IEEE 802.11az (Next Generation Positioning) [9]. In light of this, a very good opportunity has emerged in the area of indoor localisation for both urban areas and smart cities.

To further improve positioning accuracy, researchers have focused on various hybrid approaches. For 5G IoT networks, the location of the user's equipment is estimated using a combination of signal propagation characteristics such as angle of arrival (AOA), time of arrival, time difference of arrival, received signal strength (RSS), RSS difference (RSSD), direction of arrival (DOA), and frequency difference of arrival (FDoA) [3]. These hybrid approaches were recently further surveyed in [10–12]. Among all these approaches, the RSS fingerprint-based method is the most widely used for real-time tracking. Additionally, most of the existing approaches consider the use of the RSS from specific radio technology. However, the offline phase of fingerprint collection requires a considerable amount of human resources and is also time-consuming, especially for complex buildings. For this reason, we propose a K-nearest-neighbours and deep neural network (K-DNN) algorithm to improve 3D indoor positioning. The contributions of this paper can be summarized as follows:

- A realistic information fusion scenario for 5G IoT networks was planned and deployed utilizing a 5G IoT gateway, a Bluetooth Low Energy (BLE) network, and a set of wireless IoT access points without requiring any extra information such as a magnetic-inductive sensor, acoustics, visible light, or a powerline.
- Our implementation used a novel data-augmentation concept for a received signal strength (RSS)-based fingerprint technique to produce a 3D fused hybrid fingerprint. This concept was supported by the interquartile range (IQR) method for the detection and elimination of outliers.
- To improve 3D positioning accuracy, a K-DNN cooperative algorithm was implemented on the constructed hybrid multi-layered radiomap.

The concept presented is a continuation of our previous work in [13,14] towards cooperative localisation. This paper is divided into the following parts: Section 2 covers the state of the art in fingerprint-based techniques for 3D/2D positioning and information fusion methods. The proposed system model and the underlying algorithms are presented in Section 3. The 5G IoT physical network environment is explained in Section 4. The experimental setup is covered in Section 5. Section 6 provides the performance evaluation, and Section 7 analyses the obtained results. Finally, a summary and directions for future work are presented in Section 8.

2. State of the Art

2.1. Received Signal Strength

Received signal strength (RSS) is a way to measure the signal power received by a user's equipment. This is expressed in decibel milliwatts (dBm) or milliwatts (Mw). The RSS-based method is one of the methods widely adopted by the indoor localisation research community. RSS can be used to approximate the distance between a user device (UE) and a transmitting device (Tx), as shown in Figure 1.

Using an RSS indicator (RSSI), a relative measurement of RSS, and a free-space path loss (FSPL) propagation model [15], the distance delta between a UE and Tx can be estimated via the formula below:

$$FSPL(dB) = 20log_{10}(d) + 20log_{10}(f) + \phi \quad (1)$$

where d is the distance expressed in metres; f is the frequency measured in kilohertz, megahertz, or gigahertz; and ϕ is a constant based on the frequency unit. During location determination, this formula assumes that the antennas are lossless and their polarisation is the same. However, this is not often the case in complex and unpredictable environments with continuous noise.

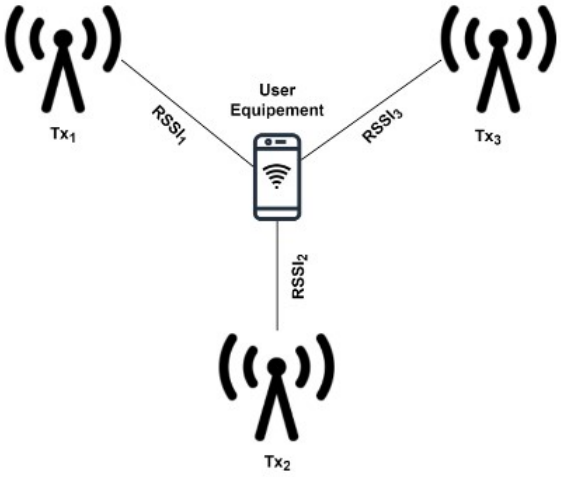

Figure 1. RSS-based positioning.

2.2. RSS Fingerprint-Based 2D and 3D Indoor Positioning

In the RSS fingerprint-based method, unlike the free-space path loss (FSPL) model, the location is estimated by matching the signal received from the user equipment with a database of preconstructed location radiomaps. The most significant advantage of this method is its ability to maintain high accuracy in a cluttered multi-path environment, according to a study conducted by [16,17]. As shown in Figure 2, this technique has two phases: offline and online. In the offline phase, a site survey or measurement campaign is conducted through which a set of RSS signals is collected and linked to its corresponding location XY in the 2D case and XYZ in the 3D case. The constructed radiomap is then used to train a localisation algorithm with a distance error loss function, such as least squares [18], weighted least means [19], maximum likelihood estimation [20], or convex optimisation [21].

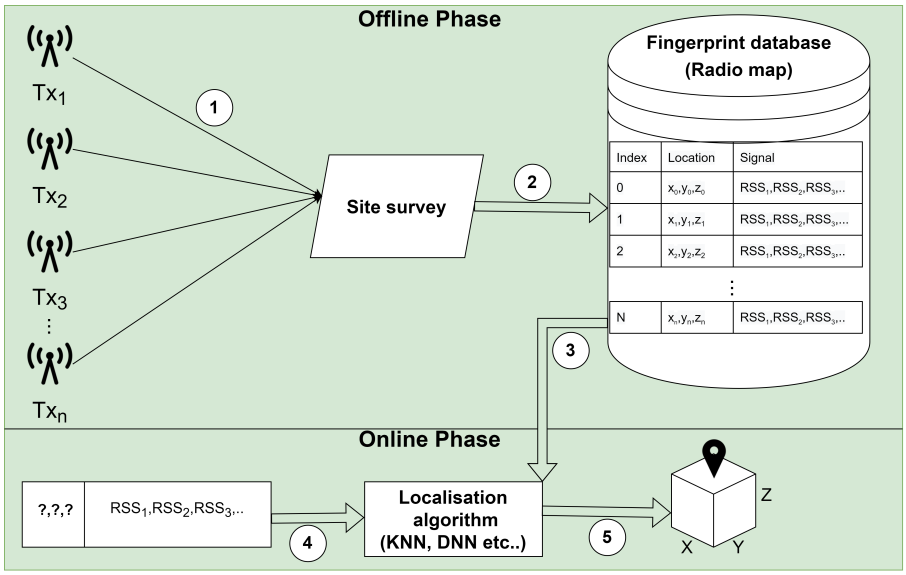

Figure 2. Fingerprint -based positioning phases.

To construct a radiomap, the most commonly used method for collecting signal fingerprints is called war-diving [22]. After identifying the indoor area of interest, the user equipment stays in each position for a specific time interval to obtain enough fingerprint information. As the monitoring device moves along the grid, the collected RSS single is stored in the database along with a reference point. Regarding 5G IoT positioning indoors,

the use of this technique was investigated by Huan et al. in [23]. The authors used the Kalman filter to remove the noisy RSS values. Next, a universal kriging (UK) algorithm was used for spatial interpolation and data augmentation to reduce dependency on the fingerprinting database. Finally, the authors trained a KNN model to calculate the user equipment's location, achieving a 1.44 m positioning error. Although this approach is interesting, it was not established whether the system could perform equally in a 3D environment. Additionally, the use of a single base station might seem to save power, but it does not guarantee the same accuracy given the changes in the environment and the LOS issues in cluttered space. Similarly, Gong et al. [24] suggested a two-step KNN (2-KNN) algorithm that used reference signals from the state information of the channel (CSI). During the offline phase, a smooth rank sequence (SRS) estimated the number of received signal paths. During the online phase, a trained 2-KNN algorithm was used to determine the 2D location of the user equipment. Most studies have overlooked 3D localisation, which is essential for scenarios like robot navigation, immersive shopping, and virtual reality. This was the main motivation for us to investigate this area. Further studies on 5G and beyond (6G) can be found in the following survey papers: [25,26].

2.3. Information Fusion for 5G IoT

Information fusion for 5G IoT has attracted considerable attention from the research community. This technique, as shown in Figure 3, involves blending data from various sources or sensors using a data fusion system to gain better inference and improve accuracy/precision. This concept produces an effective and reliable IPS (indoor positioning system) while saving the cost of expensive infrastructure [27]. Over the last decade, researchers have attempted to merge data readings from sources such as RFID [28], GPS [29], pedometers [30], BLE (Bluetooth Low Energy) [14], VLC (visible light communication), and many other technologies, as stated in [13,31]. Very recently, Klus et al. [32] examined fusing GNSS with WLAN data in a 5G network to improve positioning. The authors implemented a neural network as their main algorithm. Based on the authors' conclusions, the proposed approach achieved an accuracy of 1 m in an open space and 3.4 m in a cluttered area. A serious limitation of this study was the GNSS's inability to penetrate walls composed of different materials, especially in complex environments. In a more recent work, Alvarez-Merino et al. [33] looked into using WiFi fine-time measurement (FTM), UWB, and cellular-based radio fusion to improve indoor location accuracy. The authors' approach showed promising results. However, unlike [32], this system did not rely on existing infrastructure but required a UWB setup that could be costly and was limited to user equipment with this capability. These limitations motivated us to propose a cost-effective setup based on BLE and WiFi. A detailed discussion of these techniques can be found in the following resources: [34–36].

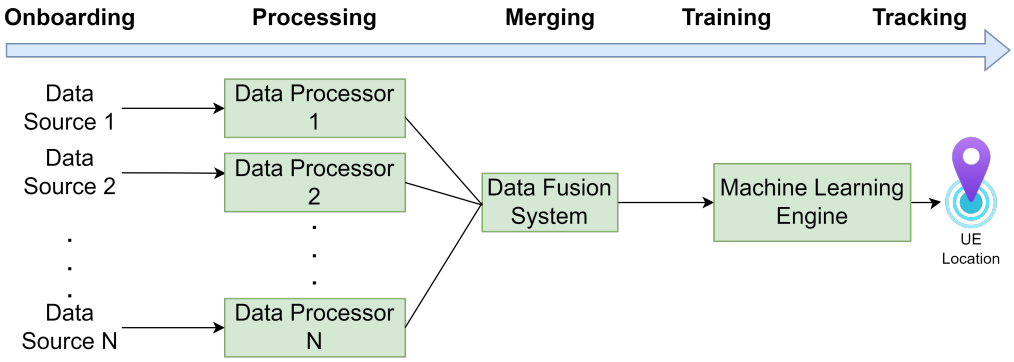

Figure 3. Information fusion localisation process.

BLE Technology

BLE has emerged as a low-cost wireless solution for localising people and assets, offering traditional Bluetooth protocol capabilities over ultra-low power consumption

circuits [37]. BLE-enabled devices communicate over 2.4 GHz and use 40 channels (PHY channels) divided by a 2MHz frequency gap. Channels 37, 38, and 39 are used for advertising, while the rest are used for data transfer during a connection. This technology uses a neighbour discovery process (NDP) in which a BLE-enabled device, often referred to as a "scanner", searches for nearby BLE devices called "advertisers" [38]. Once the discovery process has finished, a list of available devices is returned based on availability and RSS value. According to the core specification, BLE 5.0 has improved drastically compared to version 4.2, offering two types of discovery process: basic and advanced [39]. Recently, BLE has become a central source of information fusion amongst the research community. Several research papers have explored the use of this technology to improve indoor localisation accuracy. Kanakareja et al. [40] investigated using the BLE protocol along with LoRa to reduce the distance error of an indoor tracker called "The Things Network" (TTN). The idea is very promising; however, it only works for environments where a low-power wide area network (LP-WAN), like a wireless sensor network, is deployed. To track the movements of elderly people indoors, Kolakowski et al. [41] used BLE and ultra-wide band technologies. While this is a very effective low-power solution, realising it requires the deployment of UWB infrastructure. Additionally, UWB suffers from clock synchronisation issues due to the time-sensitive nature of its pulses, which is not practical for real-time localisation systems [42]. Finally, to label areas like parking lots and meeting rooms with localisation information, Hu et al. [43] proposed a system called Grid-Loc that combined both active radio frequency identification (RDFID) and BLE. Similarly, this solution needed a pre-setup to start tracking and did not make use of widely existing infrastructure technologies such as wireless local-area networks (WLANs). In our work, to improve 3D localisation, we implemented a fusion of BLE and the ubiquitous WLAN. This concept is further discussed in Section 3.

2.4. Machine Learning

In the fingerprint-based localisation method, the application of machine learning involves training a model on a radiomap dataset that has been collected during the offline phase. Given a radiomap database, the localisation model aims to infer the state or location of the user's device from the received measurement vector σ, which includes RSS values σ_i from several access points. According to the literature, the widely used algorithms can be classified into deterministic and probabilistic algorithms. The principle behind these methodologies is based on searching a database of fingerprints and finding one or more locations whose RSS values have the highest similarity to the one currently observed.

2.4.1. Probabilistic Approach

In the probabilistic approach, the position is determined based on the likelihood that the user is in the location 'x' given vector or RSS values received during the online phase. Assuming that a set of location candidates L is $L = \{L_1, L_2, L_3, ..., L_m\}$ for any obtained RSS vector values σ, one selects L_i if

$$P(L_i|\sigma) > P(L_j|\sigma) \text{ for } j,k = 1,2,3,...n, \ i \neq j \tag{2}$$

where $P(L_i|\sigma)$ is the probability that a user device is at location L_i given the RSS vector σ if its likelihood is higher than that of $P(L_j|\sigma)$.

Finally, using Equation (2), the 3D location $(\hat{x}, \hat{y}, \hat{z})$ can be estimated using the weighted average probability as follows:

$$(\hat{x}, \hat{y}, \hat{z}) = \Sigma_{i=1}^{n}(P(L_i|s)(x_{L_i}, y_{L_i}, z_{L_i})) \tag{3}$$

2.4.2. Deterministic Approach

In the deterministic positioning approach, location λ is considered a non-random vector [44]. The main objective is to estimate $\hat{\lambda}$ at every step. Usually, the location estimate

is treated as a linear combination of calibrated points p_i. The principle behind this approach can be summarised in the following equation:

$$\hat{\lambda} = \Sigma_{i=1}^{k} \frac{w_i}{\Sigma_{j=1}^{M} w_j} \lambda_i \tag{4}$$

Here, the set $\{\lambda_1 \dots \lambda_i\}$ denotes the sequence of reference points associated with Δ_i, which is the distance between the respective radiomap fingerprint $\bar{r}_i$ and the measurement x taken during live positioning, i.e., $\Delta_i = ||x_i - \bar{r}||$. The norm $||.||$ in this equation can be any arbitrary formula. This can be the Mahalanobis norm [45], the Manhattan norm (1 norm) [46], or the Euclidean norm (2 norm) [44]. As this paper focusses on the latter, w_i can be written as follows:

$$\Delta_i = \sqrt{\sum_{j=1}^{N} x_{ij} - s_j)^2} \tag{5}$$

In Equation (4), w_i is a set of non-random weight coefficients assigned to each reference point based on its importance in distinguishing it from other fingerprints. Consequently, the value of w_i assigned to each fingerprint impacts the location estimation. In this case, the weight allocation expressed in Equation (4) refers to the weighted K-nearest neighbours (WKNN) algorithm [46]. A possible value for w_i can be the inverse of the RSS innovation [46], which can be expressed as follows:

$$w_i = \frac{1}{||x - \bar{r}||} \tag{6}$$

If Equation (4) is simplified, it can be assumed that all fingerprints are assigned equal weights. As a result of this assumption, w_i is eliminated, and the formula becomes the K-nearest neighbours (KNN) method. Thus, setting K = 1, the equation yields the simple nearest neighbours (NN) method [44,47]. In terms of performance, it was demonstrated in [44,46] that the KNN and WKNN methods offer a higher degree of accuracy than the NN method in the cases of K = 3 and K = 4, respectively. However, the NN method appears to perform satisfactorily and offers the same results in the presence of high-density RSS radiomaps [48].

Several researchers have addressed the question of indoor localisation in 5G networks using KNN [23,24,49–53]. Despite this, the KNN method alone failed to deal with a highly dense 3D radiomap, as studied in [13,54,55]. This motivated us to propose a combination of deep learning and KNN methods to improve localisation in complex 3D environments. Since the main focus of this paper is on the deterministic positioning approach based on deep learning and K-nearest neighbours, more complex methods such as the database correlation method (DCM), linear discriminant analysis (LDA), and the *k*-anonymity method can be found in [56–58], respectively. The following subsection deals with existing research contributions related to deep learning.

2.4.3. Deep Learning

Deep learning is a subclass of machine learning algorithms based on artificial neural networks (ANNs) and representation learning [59]. Artificial neural networks themselves were inspired by biological networks. These types of algorithms are more powerful than traditional machine learning algorithms as they use multiple connected layers to extract complex patterns from raw data [60]. The training technique used in deep learning can be supervised, semi-supervised, or unsupervised [61]. In 5G networks, the adaptation of these techniques [62,63] in indoor and outdoor localisation has shown some great results. Wafaa et al. [64] studied the use of CNNs to reduce localisation error and improve accuracy. Their approach converted a 2D fingerprint radiomap and its kurtosis values to a 3D RSS radio image. This 3D tensor was then used as an input for their proposed model. This localisation framework was tested in a 20 m $\times$ 20 area. The reported results suggest

that this concept could achieve up to 94.13% accuracy in a grid size of 2 m × 2 m with 10 anchors. Although it sounds promising, this concept has not been tested in a 3D environment. Similarly, Yang et al. [65] proposed an indoor 3D localisation scheme based on a 1D CNN and BLE signal fingerprinting. This approach was tested in a 3D space of 4.0 m × 2.0 m × 3.0 m. The authors deployed eight BLE beacons and divided the 3D space into 16 grids of 1 m × 1 m × 1 m in size. Following these steps, the system was able to achieve a 0.25 m error and a precision of almost 100%. A serious limitation of this work was that the framework was tested in a small and uncluttered environment. Furthermore, to achieve the same result, according to the adopted setup, a BLE must be deployed for each 1 m^2. This is usually not cost-effective, especially for large complex buildings. To overcome these two limitations, we suggest the use of a hybrid radiomap and a combination of KNN and DNN to realise a cost-effective scalable solution. The following section covers the proposed approach in detail.

3. The Proposed Approach

Our proposed approach aimed to improve indoor positioning using several 5G IoT wireless signal data sources. This could be achieved by merging actual BLE and WiFi 3D location data with simulated BLE and WiFi location data into a multi-layered hybrid radiomap to save the tedious time spent constructing a fingerprint database. To support this data augmentation approach, K-DNN, a new cooperative positioning algorithm that combines KNN (K-nearest neighbours) and DNNs (dense neural networks) was developed to reduce the localisation error. Figure 4 provides an overview of the algorithmic flow of the proposed K-DNN system. The following subsections describe in detail the K-DNN algorithm used in this paper.

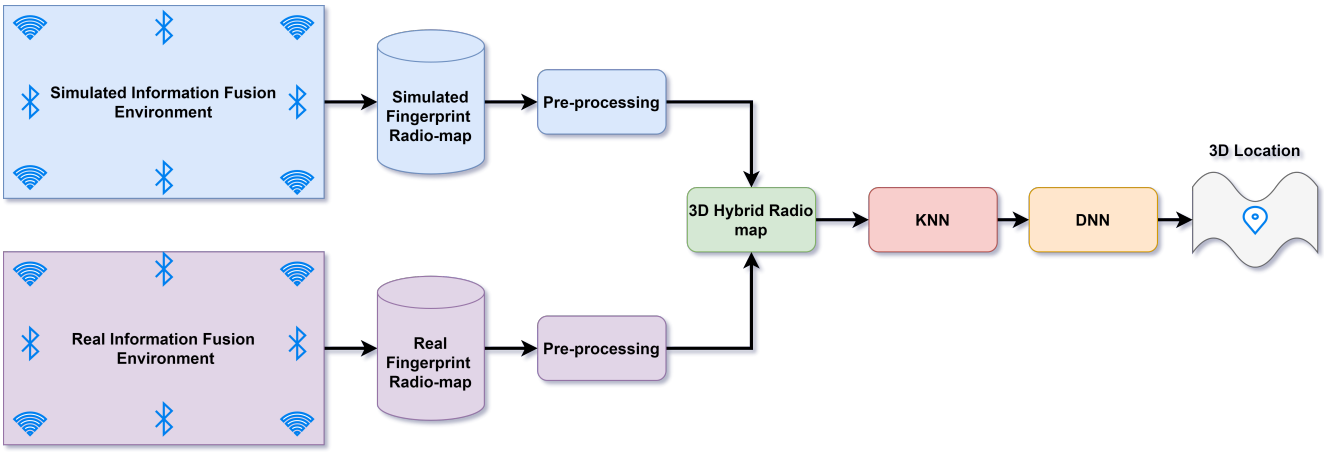

Figure 4. The flow of the proposed K-DNN system model.

3.1. K-DNN Architecture and Hybrid 3D Localisation for 5G IoT

K-DNN is a novel cooperative positioning algorithm. Given a set of WLAN transmitters N and a set of BLE transmitters M connected to a set of 3D locations (XYZ), two machine learning models are trained to support each other to achieve minimal distance error. During the offline phase, the algorithm receives two matrices of hybrid radiomaps. This can be mathematically expressed as

$$BLE\_RSS : \{(x_1, y_1, z_1, ble_1 \ldots ble_m), \ldots, (x_i, y_i, z_i, ble_1 \ldots ble_m)\}$$
$$WLAN\_RSS : \{(x_i, y_i, z_i, wlan_1 \ldots wlan_n), \ldots, (x_i, y_i, z_i, wlan_1 \ldots wlan_n)\}$$

K-DNN begins by eliminating outliers from the given radiomaps using the IQR (interquartile) method [66]. The cleaned fingerprint datasets are then merged into a single radiomap. Next, a min–max normalisation technique is implemented to convert the RSSI values of the BLE and WLAN into the same scale. As a final step in this phase, the KNN

model is first trained to predict the 2D location (X, Y), and the DNN is trained to predict the 1D location (Z).

During the online phase, the K-DNN receives the following input:

$$BLE\_RSS_{online} : \{ble_1, \ldots, ble_m\}$$
$$WLAN\_RSS_{online} : \{wlan_1, \ldots, wlan_n\}.$$

Given this, KNN attempts to approximate the 2D (XY) locations as an output. This outcome is then fed along with the original input received by KNN into the DNN, which in turn predicts the 1D (Z) location. As a result, the 3D (XYZ) location is realised through this cooperative prediction approach. The main reason for including these two models was the nature of the 1D (classes) and 2D (continuous values) outputs.

3.2. K-DNN Model Architecture

3.2.1. KNN

The K-nearest neighbours algorithm is a non-parametric supervised machine learning algorithm used for pattern classification and regression. This means that it does not make any assumptions about the data being analysed. Since learning in KNN is supervised, the trainer has to choose the parameters to achieve the best results. This algorithm was first proposed in 1951 by Evelyn Fix, Joseph Hodges [67], and Thomas Cover [68], who later expanded on it. In the K-DNN algorithm, KNN is used to predict the 2D (XY) location. As previously highlighted in Algorithm 1, this algorithm receives a set of RSS values as input R. This can be written as $R = [RSS_1, RSS_2, \ldots, RSS_n]$

The input provided to KNN consists of a vector of seven normalised RSS values. This part of K-DNN model attempts to reduce the localisation error of the X and Y location using the Euclidean distance. The output of this model is then combined with the original input R and fed into the DNN model.

3.2.2. DNN

Deep learning is a crucial building block in the proposed K-DNN system. It allows the learning of complex patterns and data representations through multiple processing layers [61]. One of the most important architectures in deep learning is the deep neural network, also known as multiple-layer perceptron (MLP) or a deep feed-forward network [69]. The DNN considered in K-DNN is a classification model. Figure 5 shows the number of layers, neurones, and input and output parameters used in this model.

The input layer of this network receives transposed vectors of signal values and 2D locations. This can be expressed as

$$DNN_{input} = [X, Y, RSS_1, RSS_2, \ldots, RSS_n]^T \tag{7}$$

where X and Y are the 2D points predicted by KNN and RSS_i represents the signal value of the ith transmitter (BLE or WLAN).

The calculated result for this layer is then fed into the first hidden layer. Each input element from Equation (7) is multiplied by a specific weight vector $\vec{w}$. The product of this operation is then added to a bias b. The formula for this can be expressed as follows:

$$h1 = \sum_{i=1}^{n} w_i^1 I_i + b_i^1 \tag{8}$$

where I_i is the element ith of the input vector. The summation of all these inputs is then passed onto an activation function unit A. In our proposed network, this is the rectified linear unit (ReLu).

$$A_1 = max(0, h1) \tag{9}$$

Here, A_1 is the activation function of the first hidden layers. The output of this layer is 128 neurones. In the same way,

$$h2 = \sum_{i=1}^{n} w_i^2 a_i^1 + b_i^2 \tag{10}$$

The result of this hidden layer is passed onto a further activation unit A_2:

$$A_2 = max(0, h2) \tag{11}$$

Finally, the output of Equation (11) is received by hidden layer 3 to make a similar calculation for $h1$ and $h2$:

$$h3 = \sum_{i=1}^{n} w_i^3 a_i^2 + b_i^3 \tag{12}$$

The values calculated by Equation (12) are then fed into the activation function below:

$$A_3 = max(0, h3) \tag{13}$$

To predict the correct height of the mobile device, the softmax function equation below is used:

$$\theta(a_i) = \frac{\exp(a_i^3)}{\sum_j \exp(a_j^3)} \tag{14}$$

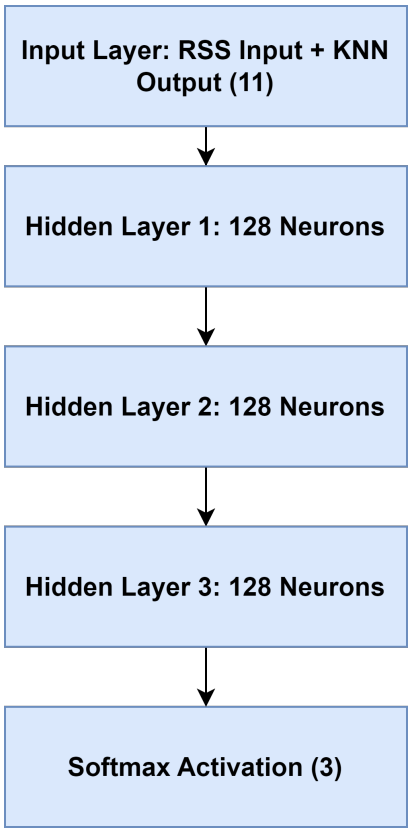

Figure 5. Layers of the DNN.

3.3. K-DNN Psuedocode

For clarity purposes, the Algorithm 1 below explains how K-DNN works.

Algorithm 1: K-DNN Algorithm for 3D Localisation

Input : $BLE\_RSS : \{(x_1, y_1, z_1, ble_1 ... ble_m)\}$; ▷ Get Hybrid BLE RSS
Input : $WLAN\_RSS : \{(x_1, y_1, z_1, wlan_1 ..... wlan_n)\}$; ▷ Get Hybrid WiFi RSS
Output: Λ ; ▷ Output 3D location
Require: Signal UpperThreshold μ;
Require: Signal LowerThreshold η;
Require: First quartile Q_1;
Require: Third quartile Q_3;
$IQR \leftarrow Q_3\text{-}Q_1$; ▷ Calculate Interquartile
for ble_i *in BLE_RSS and* $wlan_i$ *in WLAN_RSS* **do**
  if $ble_i < Q_3 + (1.5 * IQR)$ ***and*** $ble_i > Q_1 - (1.5 * IQR)$ **then**
    $ble\_r \leftarrow ble_i$; ▷ Apply IQR method to BLE
  if $wlan_i < Q_3 + (1.5 * IQR)$ ***and*** $wlan_i > Q_1 - (1.5 * IQR)$ **then**
    $wlan\_r \leftarrow wlan_i$; ▷ Apply IQR method to WLAN
  $RSS \leftarrow wlan\_r \cup ble\_r$; ▷ Fuse BLE and WLAN Radiomaps
end
for RSS_i *in RSS* **do**
  $R \leftarrow \frac{RSS_i - \mu}{\mu - \eta}$; ▷ Normalize signal
  $X\_Y \leftarrow KNN(R)$; ▷ Apply first model prediction
  $Z \leftarrow DNN(R, X\_Y)$; ▷ Apply second model prediction
  $\Lambda \leftarrow X\_Y \cup Z$; ▷ merge results output
end
return Λ

4. 5G IoT Physical Network Environment

In this part of the article, we explain the main components of the 5G IoT network that was used in this experiment. For clarity purposes, Figure 6 shows the logical network architecture.

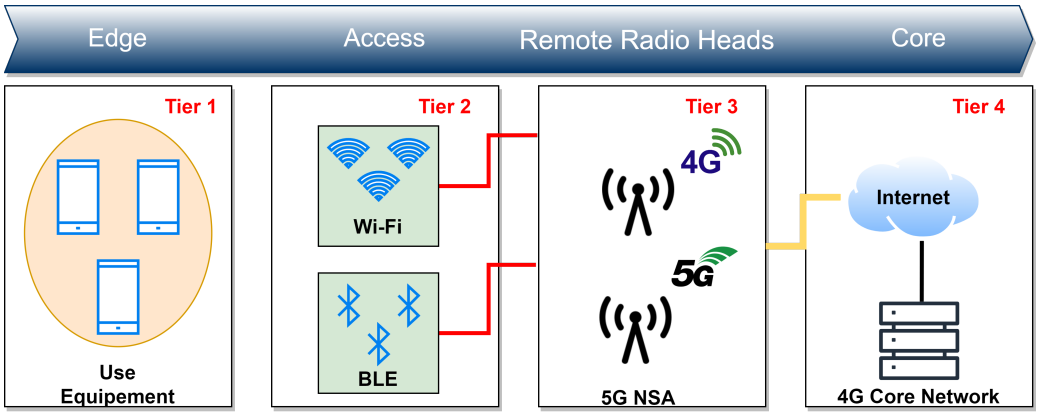

Figure 6. 5G IoT network logical architecture.

4.1. 5G Core Network

In this experimental testbed, we adopted 5G NSA (non-stand-alone) access as suggested by 3GPP release 15 [70]. This concept uses dual connectivity (eNodeB/gNodeB) to provide radio access to 5G-enabled UE (user equipment) via 4G EPC infrastructure, as demonstrated in Figure 7a. The 5G core network complied with 3GPP release 16 [71] and used an open source called Open5gs [72]. This platform implements both 5GC (5G core) and EPC (evolved packet core) using the C language. Open5G has evolved from

4G NextEPC and comes with a WebUI to manage network subscribers. The developed 5G core network was used to configure NR/LTE networks for a private cellular network infrastructure. The core network was virtualised and deployed on a 64-bit Linux machine using a VMWARE workstation. It is worth mentioning that at the time of writing this paper, other projects such as OpenAirInterface [73] and free5GC [74] have been instigated. However, these solutions are not stable yet. A detailed description of these three projects can be found in [75].

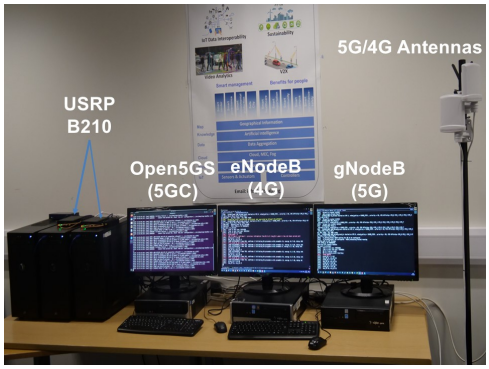

(**a**) 5G lab setup

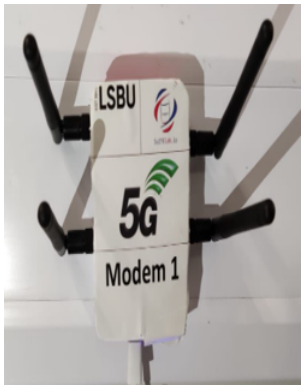

(**b**) 5G modem gateway

(**c**) Bluetooth Low Energy 2

(**d**) 5G wireless access point 4

Figure 7. 5G IoT test environment.

4.2. eNodeB (4G)/gNodeB (5G)

The Evolved/E-UTRAN Node B is a component in the E-UTRA of 4G LTE11. This component connects subscribers to service providers through the S1-AP protocol linked to S1-MME from the mobility management entity side. The eNodeB has its own radio control functionality that manages a USRP B210 SDR (software-defined radio), as shown in Figure 7a. This component offers a radio service via the air interface. The operating frequency of this radio unit for 4G is between 800 MHz and 2600 MHz, as per the OfCom regulations. A duplexer was also used to reduce the number of antennas needed to keep the transmitter (Tx) and receiver (Rx) synchronised for both radio units. The software side of this solution was implemented on a custom-built PC powered by an i9 CPU with a total memory of 32 GB. This unit was an implementation of 3GPP release 15 [70], as previously highlighted. This meant that it used dual connectivity to offer the service to the user equipment. The 5G-capable device had to first connect to the MME through the eNodeB to attach to a gNodeB. This is why it is called the NSA mode. This unit used the X2AP protocol to communicate with the eNodeB nearby. The dedicated hardware for this base station was similar to the eNodeB. In order to reduce the clock drifting, a 5G radio was offered through a USRP B210 attached to a 5G band 7 cavity duplexer.

4.3. 5G IoT Modem

The 5G gateway implemented in this testbed consisted of a Raspberry Pi 4 model B and a Quectel 5G Quectel RM500Q-GL modem [76], as shown in Figure 7b. This gateway linked the 5G cellular network to the WLAN and BLE networks used to extract fingerprints.

4.4. Wireless Local Area Networks

During the experimental design, five IEEE 802.11ac [77] wireless access points were considered for deployment at the assigned site. Figure 7d depicts one of the access points used in this setup. In this configuration, each transmitter operated at 2.4 Ghz and a coverage range of 45 m, although dual band was possible, as this technology also supports 5 Ghz.

4.5. Bluetooth Low Energy

As a secondary source for information fusion, we considered using the IEEE 802.15.1 standard, which is BLE version 5.0 [78]. The devices used in this experiment operated at 2.4 Ghz and 350 m. Figure 7c illustrates one of the BLE units used in this setup. The following section covers the simulated environment of this architecture.

5. Test Environment

The K-DNN algorithm was tested by combining actual and simulated measurements. The experiment took place in two teaching laboratories at London South Bank University of approximately 126 m^2 (6 m wide by 21 m long by 3 m high), as shown in Figure 8.

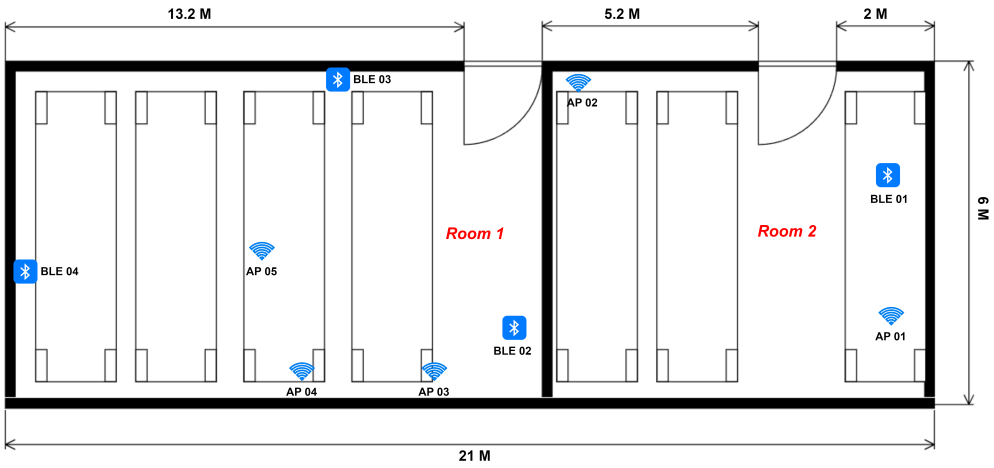

Figure 8. Floor plan with access points and BLE position.

To achieve this task, a 5G IoT network was deployed in the two laboratories. The network consisted of five IEEE 802.11 access points and four IEEE 802.15 BLE units that were randomly placed based on Table 1. Two radiomaps were constructed: the first was generated using an actual measurement campaign, and the second using TruNet wireless, a 3D ray-tracing deterministic simulator [79].

Table 1. The 5G IoT setup location and antenna orientation.

Device	X	Y	Z	Antenna Orientation
AP1	0	0	2	Vertical
AP2	6	6.5	1.5	Horizontal
AP3	0	11	1.5	Vertical
AP4	0	13	1	Horizontal
AP5	3	15	0.5	Horizontal
BLE01	4	0	1	N/A
BLE02	1	9	1.5	N/A
BLE03	6	13	2	N/A
BLE04	3	21	0.5	N/A

5.1. Radiomap from Actual 5G IoT Measurements

During data collection, fingerprints were collected in 2236 equally spaced locations (0.5 m spacing) at 0.5 m, 1 m, 1.5 m, and 2.5 m heights, as shown in Figure 9a. At each measurement location, 30 distinct measurements were recorded at an interval of 1 second using the iFused fingerprint data collector developed for Android-based devices, as shown in Figure 9b. The RSS values stored in the radiomap ranged from −103 dBm to −28 dBm. During the measurement campaign, the application recorded data from 5 APs and 4 BLE devices.

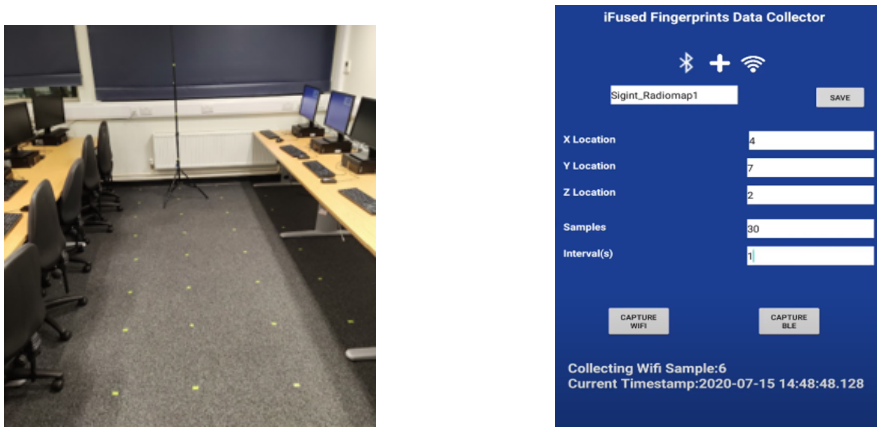

(**a**) FW-208 classroom grid setup (**b**) iFused fingerprint data collector

Figure 9. Physical environment and fingerprint data collector.

5.2. 5G IoT Simulated Radiomap

5.2.1. TruNet Tool

As previously highlighted, we considered using a 3D ray-tracing (RT) deterministic tool called Trunet [79]. This application constructs 3D radiomaps in conjunction with calibration techniques. The main advantage is that the tool generates efficient radiomaps while saving the time and cost incurred by a measurement campaign. Figure 10a,b illustrate the building simulated using the Trunet software along with a layer of the multi-layered simulated radiomap generated for both WLAN and BLE, respectively.

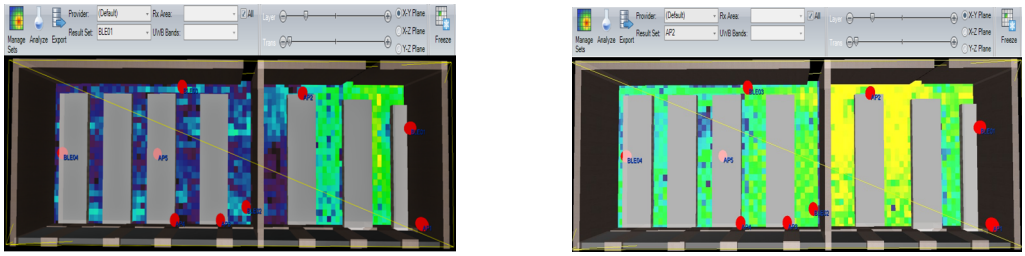

(**a**) Simulated radiomap for BLE 1 (**b**) Simulated radiomap for access point 2

Figure 10. 5G IoT simulated environment radiomap example.

5.2.2. Simulated Radiomap

The second radiomap was constructed using the TruNet simulator. RSS fingerprints were collected according to the procedure used by the authors of [13,80]. To ensure that the measurement recorded by the iFuse application matched the simulated measurements, 5 APs and 4 BLE units were configured according to the antenna radio propagation characteristics in Table 2. Furthermore, the building structure and furniture were configured based on the calibration procedure in [81]. As a result, the same 2236 measurement points were generated and defined as receiver cells. At the end of this process, two layers of fingerprints (2 m and 1.5 m high) were merged with the actual measurement radiomap.

Table 2. The BLE and WLAN radio propagation parameters.

Parameter	BLE	WLAN
Rx sensitivity (dBm)	−70	−120
Tx power (dBm)	8	12
Antenna type	Omnidirectional	Omnidirectional
Max refractions	5	12
Max reflections	5	12
Max diffractions	1	1

5.2.3. The physical Network Behaviour

It was evident that the obtained RSS signal could be affected by various types of noise from the environment. We needed to ensure that the radiomap constructed by the simulation matched with the results of the measurement campaign. Figure 11 shows a strong correlation between the real RSS values and the Trunet values measured for access points and BLE units.

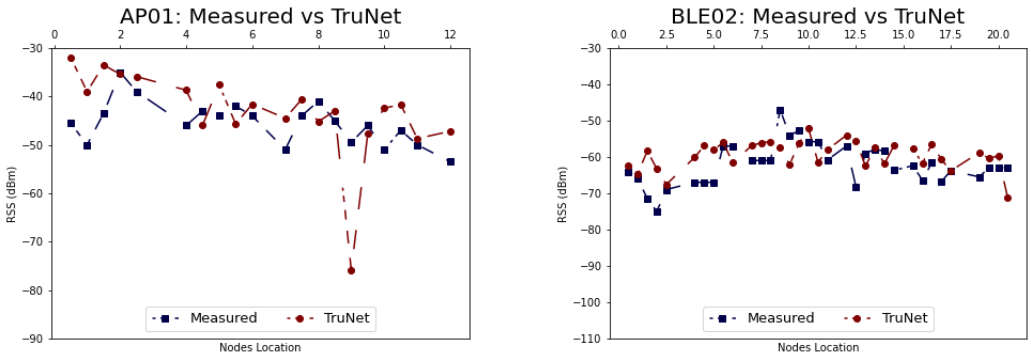

(**a**) Measured vs. simulated fingerprints for AP 01 (**b**) Measured vs. simulated fingerprints for BLE 02

Figure 11. BLE 02 and AP 01 simulated vs. real measurement comparison.

5.3. Preprocessing

5.3.1. Multi-Layered Radiomap Hybridisation

The hybridisation of a radiomap refers to the process of merging simulated and real measurements of the same environment at different height levels. This preprocessing technique merges multiple 3D layers from various available sources. In this experiment, we combined two simulated measurements (2 m and 1.5 m heights) with two layers of real measurements (0.5 m and 1m heights). This technique is novel as far as we know and has not been implemented in previous papers. It could be beneficial for scenarios involving complex buildings where extensive human resources and time are allocated. To ensure that there was a correlation between the simulated and real measurements, we compared the location IDs of the same layer belonging to the same BLE and access point. As demonstrated in Figure 12, there was a strong correlation between the measurements obtained in the simulation and the actual measurements. Furthermore, to prove the feasibility of this technique, we compared the non-fused and fused models, as presented at a later stage in this paper.

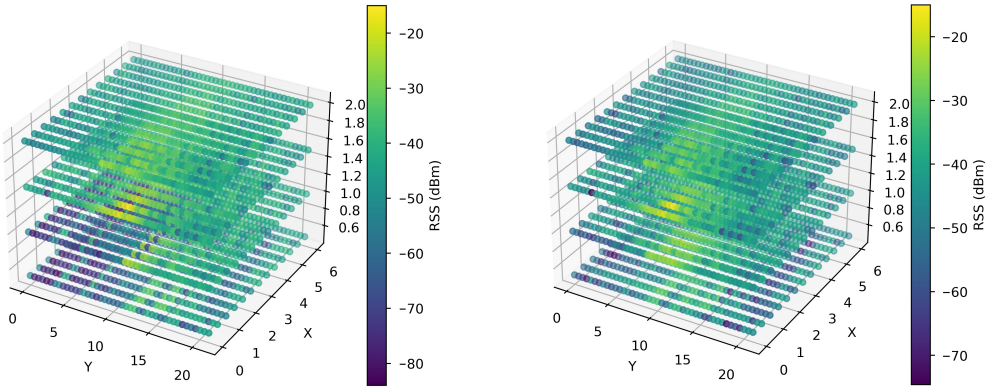

(**a**) Access point 03 hybrid radiomap (**b**) Access point 03 simulated radiomap

Figure 12. Simulated Authors. No need to move it. vs. hybrid radiomap.

5.3.2. Feature Selection

During the feature selection process, a Pearson correlation test was performed between the BLE units and APs, as this was necessary to ensure that there was no redundancy in the information provided to the K-DNN models. Figure 13 clearly shows that there was no substantially positive or negative correlation between the selected BLE unit and AP used in this experiment.

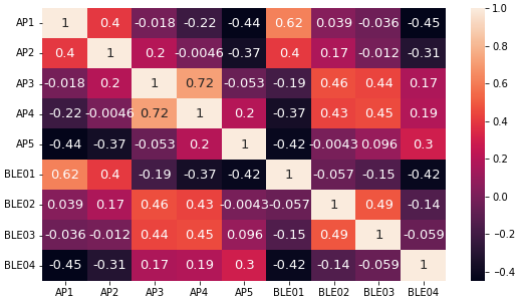

Figure 13. Pearson correlation matrix for the radiomap.

5.3.3. Outlier Elimination

Outliers are generally values that lie an abnormal distance from other values in a normal distribution. In the case of RSS-based positioning, these types of values find their way into a radiomap during the measurement campaign when a signal fluctuation occurs or

when there is interference, such as human activity. To deal with this data quality problem, we applied the interquartile method introduced by Upton and Cook in [82], as shown in Figure 14.

In this work, we implemented this method to prevent K-DNN from learning extreme RSS values that were picked up by the receiver during the data collection process. After treating the outliers, 2031 observations were left to train the K-DNN model. Table 3 shows a summary of the considered features and their minimum and maximum values.

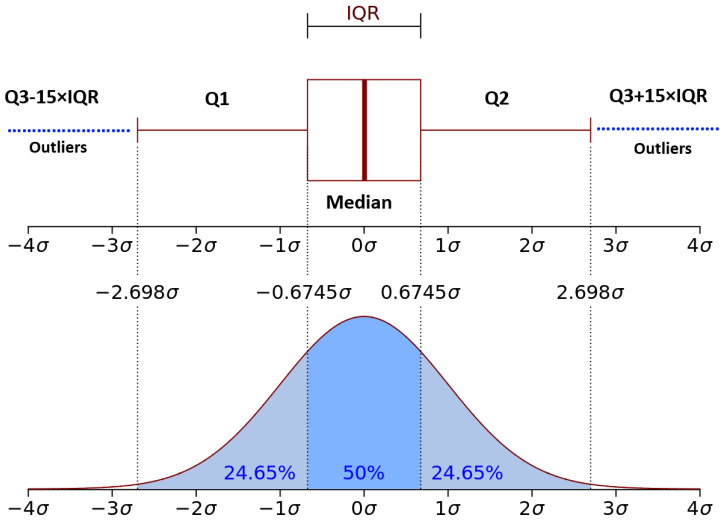

Figure 14. Outlier removal using IQR technique.

Table 3. The features used to construct the fingerprint database.

Variable	Min. Value	Max. Value	Type
X	0	6	Coordinates
Y	0	21	Coordinates
Z	0.5	2	Coordinates
AP1	−84 dBm	−28 dBm	RSS value
AP2	−86 dBm	−30 dBm	RSS value
AP3	−84 dBm	−35 dBm	RSS value
AP4	−87 dBm	−32 dBm	RSS value
AP5	−109 dBm	−37 dBm	RSS value
BLE01	−105 dBm	−32 dBm	RSS value
BLE02	−86 dBm	−32 dBm	RSS value
BLE03	−97 dBm	−35 dBm	RSS value
BLE04	−120 dBm	−42 dBm	RSS value

5.3.4. Data Normalisation

To preserve the relationship between the original data values while speeding up the learning process, a min–max normalisation technique was implemented to scale the original values between 0 and 1. Since the scaled values were negative, we extracted the absolute value. The equation used was

$$\left| \frac{RSS_i - min(RSS)}{min(RSS) - max(RSS)} \right| \quad (15)$$

where $min(RSS)$ refers to the minimum value of the threshold signal in the training signal, that is, −120 dBm, and $max(RSS)$ represents the maximum measured value, that is, −28 dBm. Each measurement of the signal that we needed to convert is denoted by RSS_i, where i is the ith row on the N BLE unit or access point transmitter. For a different scenario, it would be preferable to rely on the receiver sensitivity level as the minimum value while choosing the strongest measured signal value during the offline phase as the maximum value. This process was important for both the KNN and DNN models, as it changed the values of each access point and BLE unit to a common scale, without affecting the differences in the range of values.

5.3.5. One-Hot Encoding

One-hot encoding is the process of converting a column of continuous ordinal numeric values to binary columns based on the distinctive values [13], as shown in Algorithm 2. This process was applied in this experiment to the 1D (Z) values. Mapping the distinctive values 0.5 m, 1.0 m, 1.5 m, and 2.0 m to four binary columns was the result of this process.

Algorithm 2: One-Hot Encoding

Input :Column Z ▷ `get Z columns`
Output:Result matrix of N binary vectors unique values from Z
Dictionary D = [];
Results R = {[],[],[],[]};
for *i in Z.length* **do**
  if i ∉ D:▷ `If value not in dictionary add it`
  key = D[i]
  D[i] = Z[i]
end
return D
Map D into results R columns as binary vector $\{[Z_1], [Z_2], \ldots, [Z_n]\}$

6. Performance Evaluation

Testing the performance of K-DNN involved training the DNN using the ADAM (adaptive momentum) algorithm [83] and KNN using the elbow method [84]. The former is useful for learning highly sparse datasets, while the latter is a technique used to cross-check the model performance against the number of K chosen. Figure 15a reveals how the DNN converged in the 1000th training iteration. The KNN model achieved the lowest error rate at K = 6, as illustrated in Figure 15b.

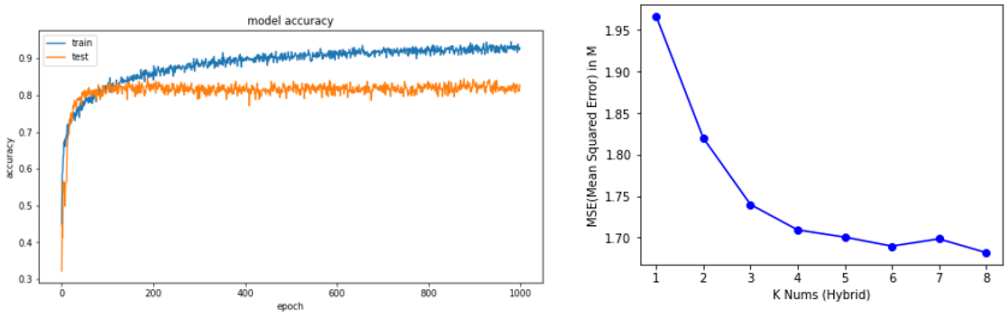

(**a**) DNN Epochs vs. model accuracy (**b**) KNN MSE vs. the number of K selected

Figure 15. 5G IoT simulated environment radiomap example.

Additionally, it is worth noting that the DNNs were trained using the hyperparameters in Table 4. In the following section, we evaluate and compare the performance of this model on different radiomaps.

Table 4. DNN hyperparameters.

Hyperparameter	Value
Learning algorithm	ADAM
Learning rate	0.001
β 1	0.9
β 2	0.999
Dropout	0.35
Momentum	0.99
Batch size	64
ϵ	1e-07
Number of hidden layers	3
Number of hidden layers in each neuron	128

7. Results Analysis

7.1. DNN Scoring

To assess the impact of the proposed approach, we trained four models using different combinations of radiomaps to draw comparisons with the concept suggested in this paper. The four models were trained as follows:

- Model 1: hybrid radiomap (proposed approach).
- Model 2: hybrid radiomap without information fusion.
- Model 3: simulated radiomap.
- Model 4: simulated radiomap without information fusion.

Using 180 random samples, as suggested by the authors in [85], we tested the misclassification performance of each DNN model at various heights: 0.5 m, 1 m, 1.5 m, and 2 m, as illustrated in Figure 16. In the graph, it is clear that the hybrid approach with information fusion achieved the lowest misclassification count out of the four models. As can be seen in Table 5, 91% of the samples—circa 164—were accurately classified. The model trained using the proposed hybrid approach without information fusion came second, with a classification rate of 87% (152 out of 180 samples). The third model was trained with information fusion and a simulated radiomap, and it performed badly compared to the two previous models. This model achieved a classification rate of 73% (132 out of 180 samples). The fourth model, which was trained using a simulated radiomap without information fusion, performed worse, with a classification score of 56 out of 180. These results demonstrate how the proposed hybrid approach outperformed the rest of the training scenarios. Given this, it could be concluded that the hybrid information fusion technique could drastically improve localisation in a 1D environment. Detailed misclassification counts for each height are provided in Table 5. The model with the poorest performance is indicated in red, while the model with the best performance is denoted in blue.

Table 5. Detailed results of DNN misclassification count.

	Hybrid	Hybrid No Fusion	Simulated	Simulated No Fusion
0.5 m	0	9	17	18
1 m	8	8	14	17
1.5 m	3	5	10	11
2 m	5	6	7	10
Total	16	28	48	56

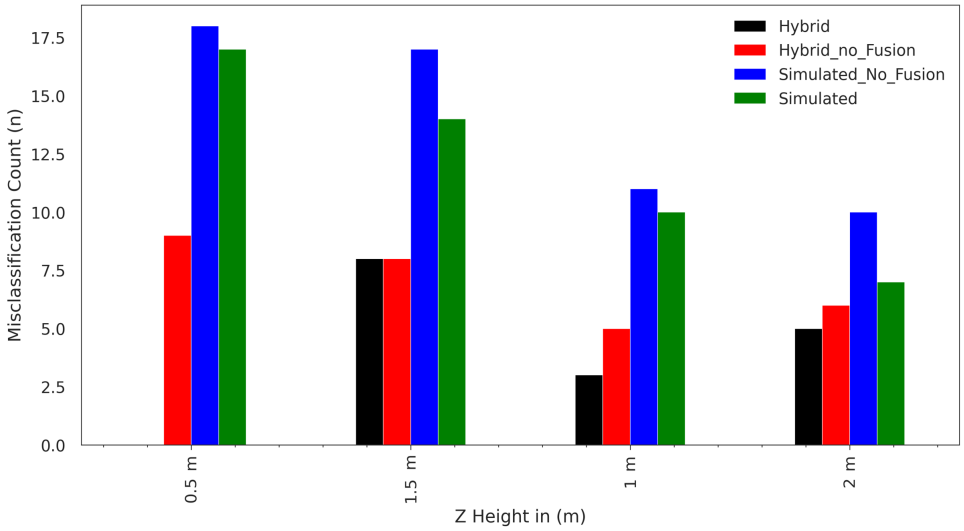

Figure 16. DNN misclassification count results by height.

7.2. KNN Scoring

As in the previous subsection, to assess the feasibility of our proposed technique in 2D localisation, four KNN models were evaluated using 180 samples. The trained models were as follows:

- KNN 1: hybrid radiomap with information fusion.
- KNN 2: hybrid radiomap without information fusion.
- KNN 3: simulated radiomap with information fusion.
- KNN 4: simulated radiomap without information fusion.

Figure 17 shows the cumulative distribution function (CDF) of the error in metres for each KNN model. For the 75th percentile, it is demonstrated that the hybrid with fusion, simulated with fusion, hybrid, and simulated models achieved 90 cm, 1 m, 1.10 m, and 1.20 m errors, respectively. Using the CDF as a metric, the proposed 3D multi-layered hybrid approach achieved a submetre accuracy, in contrast to the rest of the models. Therefore, given the results for KNN and the DNN, it can be strongly argued that the proposed K-DNN method drastically reduced the localisation error.

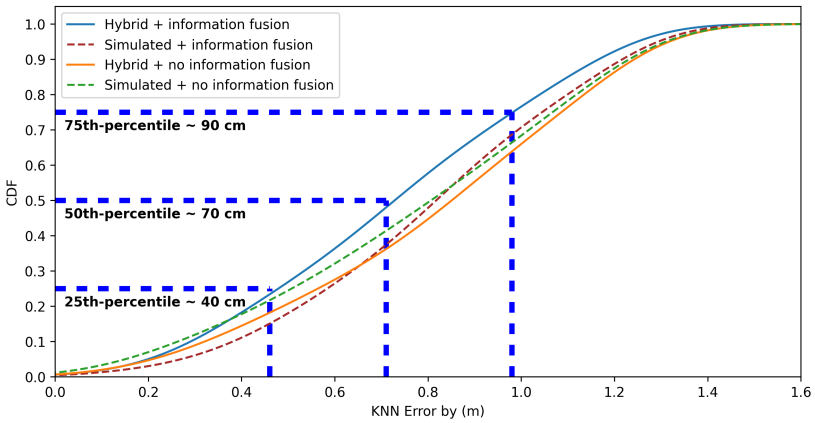

Figure 17. KNN CDF results.

8. Conclusions and Future Work

In this work, we proposed a novel algorithm for improved indoor positioning in 5G IoT networks. The proposed approach used IQR to deal with outliers and a hybrid radiomap to reduce the labour cost incurred during the data collection phase. Additionally, we demonstrated how cooperative machine learning localisation can be implemented on

top of this technique. Using this approach, we showed how information fusion implemented on 3D multi-layered radiomaps can be used to reduce the localisation error to the submetre level in 2D and attain a 91% classification rate in 1D. This result could be achieved in a similar environment if the steps in Figure 4 are followed. This concept has the potential for expansion into more intricate indoor positioning scenarios, encompassing diverse radio data sources from a heterogeneous network like 5G micro-infrastructure (including microcells, femtocells, and picocells). Additionally, our proposed K-DNN model demonstrated strong performance with RSS-based IoT and wireless sensor networks. As a result, our future endeavours will focus on enhancing the model by integrating data from different azimuth angles (45°, 90°, 180°, and 360°). Another avenue of research could involve incorporating floor-level detection for buildings with multiple stories.

Author Contributions: Conceptualization, B.E.B. and L.K.; methodology, B.E.B., L.K., T.D. and M.I.; software, B.E.B.; validation, B.E.B., L.K., T.D. and C.C.; formal analysis, B.E.B. and L.K.; investigation, B.E.B.; resources, T.D. and B.E.B.; data curation, B.E.B. and L.K.; writing—original draft preparation, B.E.B. and L.K.; writing—review and editing, L.K., T.D. and C.C.; visualization, B.E.B.; supervision, L.K. and T.D.; project administration, T.D.; All authors have read and agreed to the published version of the manuscript.

Funding: This research received no external funding.

Data Availability Statement: Not applicable.

Conflicts of Interest: The authors declare no conflict of interest.

References

1. Ge, Y.; Wen, F.; Kim, H.; Zhu, M.; Jiang, F.; Kim, S.; Svensson, L.; Wymeersch, H. 5G SLAM using the clustering and assignment approach with diffuse multipath. *Sensors* **2020**, *20*, 4656. [CrossRef]
2. Walia, J.S.; Hämmäinen, H.; Kilkki, K.; Yrjölä, S. 5G network slicing strategies for a smart factory. *Comput. Ind.* **2019**, *111*, 108–120. [CrossRef]
3. Li, G.; Lian, W.; Qu, H.; Li, Z.; Zhou, Q.; Tian, J. Improving patient care through the development of a 5G-powered smart hospital. *Nat. Med.* **2021**, *27*, 936–937. [CrossRef] [PubMed]
4. Khan, S.K.; Naseem, U.; Siraj, H.; Razzak, I.; Imran, M. The role of unmanned aerial vehicles and mmWave in 5G: Recent advances and challenges. *Trans. Emerg. Telecommun. Technol.* **2021**, *32*, e4241. [CrossRef]
5. Cisco. Cisco Annual Internet Report-Cisco Annual Internet Report (2018–2023) White Paper— Cisco. Available online: https://www.cisco.com/c/en/us/solutions/collateral/executive-perspectives/annual-internet-report/white-paper-c11-741490.html. (accessed on 10 February 2022).
6. Norris, P. Satellite Programs in the USA 59. In *Handbook of Space Security*; Springer: Berlin/Heidelberg, Germany , 2020; p. 1133.
7. 3GPP. *TR-2 2.872: Study on Positioning Use Cases*; Tech. Report 16; ETSI: Sophia Antipolis, France , 2018.
8. Wymeersch, H.; Seco-Granados, G.; Destino, G.; Dardari, D.; Tufvesson, F. 5G mmWave positioning for vehicular networks. *IEEE Wirel. Commun.* **2017**, *24*, 80–86. [CrossRef]
9. Leonardo, L.; Yuhei, N.; Kurosaki, M.; Ochi, H. High Precision Localization Protocol with Diversity for 802.11 az. *IEICE Tech. Rep. IEICE Tech. Rep.* **2017**, *117*, 69–74.
10. Alsinglawi, B.; Elkhodr, M.; Nguyen, Q.V.; Gunawardana, U.; Maeder, A.; Simoff, S. RFID localisation for Internet of Things smart homes: A survey. *arXiv* **2017**, arXiv:1702.02311.
11. Deak, G.; Curran, K.; Condell, J. A survey of active and passive indoor localisation systems. *Comput. Commun.* **2012**, *35*, 1939–1954. [CrossRef]
12. Yassin, A.; Nasser, Y.; Awad, M.; Al-Dubai, A.; Liu, R.; Yuen, C.; Raulefs, R.; Aboutanios, E. Recent advances in indoor localization: A survey on theoretical approaches and applications. *IEEE Commun. Surv. Tutor.* **2016**, *19*, 1327–1346. [CrossRef]
13. El Boudani, B.; Kanaris, L.; Kokkinis, A.; Kyriacou, M.; Chrysoulas, C.; Stavrou, S.; Dagiuklas, T. Implementing deep learning techniques in 5G IoT networks for 3D indoor positioning: DELTA (DeEp Learning-Based Co-operaTive Architecture). *Sensors* **2020**, *20*, 5495. [CrossRef]
14. Kanaris, L.; Kokkinis, A.; Liotta, A.; Stavrou, S. Fusing bluetooth beacon data with Wi-Fi radiomaps for improved indoor localization. *Sensors* **2017**, *17*, 812. [CrossRef] [PubMed]
15. Guerra, A.; Guidi, F.; Dardari, D. Single-anchor localization and orientation performance limits using massive arrays: MIMO vs. beamforming. *IEEE Trans. Wirel. Commun.* **2018**, *17*, 5241–5255. [CrossRef]
16. Liu, Y.; Shi, X.; He, S.; Shi, Z. Prospective positioning architecture and technologies in 5G networks. *IEEE Netw.* **2017**, *31*, 115–121. [CrossRef]

17. Horsmanheimo, S.; Lembo, S.; Tuomimaki, L.; Huilla, S.; Honkamaa, P.; Laukkanen, M.; Kemppi, P. Indoor positioning platform to support 5G location based services. In Proceedings of the 2019 IEEE International Conference on Communications Workshops (ICC Workshops), Shanghai, China, 20–24 May 2019; pp. 1–6.
18. Wang, G.; Chen, H.; Li, Y.; Jin, M. On received-signal-strength based localization with unknown transmit power and path loss exponent. *IEEE Wirel. Commun. Lett.* **2012**, *1*, 536–539. [CrossRef]
19. Huang, J.; Liu, P.; Lin, W.; Gui, G. RSS-based method for sensor localization with unknown transmit power and uncertainty in path loss exponent. *Sensors* **2016**, *16*, 1452. [CrossRef] [PubMed]
20. Coluccia, A.; Ricciato, F. On ML estimation for automatic RSS-based indoor localization. In Proceedings of the IEEE 5th International Symposium on Wireless Pervasive Computing 2010, Modena, Italy, 5–7 May 2010; pp. 495–502.
21. Zhang, Y.; Xing, S.; Zhu, Y.; Yan, F.; Shen, L. RSS-based localization in WSNs using Gaussian mixture model via semidefinite relaxation. *IEEE Commun. Lett.* **2017**, *21*, 1329–1332. [CrossRef]
22. Tsui, A.W.T.; Lin, W.C.; Chen, W.J.; Huang, P.; Chu, H.H. Accuracy performance analysis between war driving and war walking in metropolitan Wi-Fi localization. *IEEE Trans. Mob. Comput.* **2010**, *9*, 1551–1562. [CrossRef]
23. Huang, S.; Zhao, K.; Zheng, Z.; Ji, W.; Li, T.; Liao, X. An optimized fingerprinting-based indoor positioning with Kalman filter and universal kriging for 5G internet of things. *Wirel. Commun. Mob. Comput.* **2021**, *2021*, 9936706. [CrossRef]
24. Gong, Y.; Zhang, L. Improved K-nearest neighbor algorithm for indoor positioning using 5G channel state information. In Proceedings of the 2021 IEEE 5th Information Technology, Networking, Electronic and Automation Control Conference (ITNEC), Xi'an, China, 15–17 October 2021; Volume 5, pp. 333–337.
25. Mogyorósi, F.; Revisnyei, P.; Pašić, A.; Papp, Z.; Törös, I.; Varga, P.; Pašić, A. Positioning in 5G and 6G Networks & mdash—A Survey. *Sensors* **2022**, *22*, 4757. [CrossRef]
26. Farahsari, P.S.; Farahzadi, A.; Rezazadeh, J.; Bagheri, A. A Survey on Indoor Positioning Systems for IoT-Based Applications. *IEEE Internet Things J.* **2022**, *9*, 7680–7699. [CrossRef]
27. He, S.; Shin, H.S.; Xu, S.; Tsourdos, A. Distributed estimation over a low-cost sensor network: A review of state-of-the-art. *Inf. Fusion* **2020**, *54*, 21–43. [CrossRef]
28. Aoughlis, S.; Saddaoui, R.; Achour, B.; Laghrouche, M. Dairy cows' localisation and feeding behaviour monitoring using a combination of IMU and RFID network. *Int. J. Sens. Netw.* **2021**, *37*, 23–35. [CrossRef]
29. Aikawa, S.; Yamamoto, S.; Morimoto, M. WLAN finger print localization using deep learning. In Proceedings of the 2018 IEEE Asia-Pacific Conference on Antennas and Propagation (APCAP), Auckland, New Zealand, 5–8 August 2018; pp. 541–542.
30. Hilsenbeck, S.; Bobkov, D.; Schroth, G.; Huitl, R.; Steinbach, E. Graph-based data fusion of pedometer and WiFi measurements for mobile indoor positioning. In Proceedings of the 2014 ACM International Joint Conference on Pervasive and Ubiquitous Computing, Seattle, WA, USA, 13–17 September 2014; pp. 147–158.
31. Kanaris, L.; Kokkinis, A.; Liotta, A.; Stavrou, S. Combining smart lighting and radio fingerprinting for improved indoor localization. In Proceedings of the 2017 IEEE 14th International Conference on Networking, Sensing and Control (ICNSC), Calabria, Italy, 16–18 May 2017; pp. 447–452.
32. Klus, R.; Talvitie, J.; Valkama, M. Neural network fingerprinting and GNSS data fusion for improved localization in 5G. In Proceedings of the 2021 International Conference on Localization and GNSS (ICL-GNSS), Tampere, Finland, 1–3 June 2021 ; pp. 1–6.
33. Álvarez-Merino, C.S.; Luo-Chen, H.Q.; Khatib, E.J.; Barco, R. WiFi FTM, UWB and cellular-based radio fusion for indoor positioning. *Sensors* **2021**, *21*, 7020. [CrossRef] [PubMed]
34. Abu-Mahfouz, A.M.; Hancke, G.P. Localised information fusion techniques for location discovery in wireless sensor networks. *Int. J. Sens. Netw.* **2018**, *26*, 12–25. [CrossRef]
35. Zhang, Y.; Jiang, C.; Yue, B.; Wan, J.; Guizani, M. Information fusion for edge intelligence: A survey. *Inf. Fusion* **2022**, *81*, 171–186. [CrossRef]
36. Zhuang, Y.; Sun, X.; Li, Y.; Huai, J.; Hua, L.; Yang, X.; Cao, X.; Zhang, P.; Cao, Y.; Qi, L.; et al. Multi-sensor integrated navigation/positioning systems using data fusion: From analytics-based to learning-based approaches. *Inf. Fusion* **2023**, *95*, 62–90. [CrossRef]
37. Ji, T.; Li, W.; Zhu, X.; Liu, M. Survey on indoor fingerprint localization for BLE. In Proceedings of the 2022 IEEE 6th Information Technology and Mechatronics Engineering Conference (ITOEC), Chongqing, China, 4–6 March 2022; Volume 6, pp. 129–134.
38. Shan, G.; Choi, G.; Roh, B.H.; Kang, J. An Improved Neighbor Discovery Process in BLE 5.0. In Proceedings of the 2019 IEEE 10th Annual Information Technology, Electronics and Mobile Communication Conference (IEMCON), Vancouver, BC, Canada, 17–19 October 2019; pp. 0809–0812.
39. Core Specification 5.0–Bluetooth® Technology Website. Available online: https://www.bluetooth.com/specifications/specs/core-specification-5/ (accessed on 10 May 2022).
40. Kanakaraja, P.; Kotamraju, S.K.; Nadipalli, L.S.P.S.; Aswin Kume, S.W. IoT enabled BLE and LoRa based indoor localization without GPS. *Turk. J. Comput. Math. Educ. (TURCOMAT)* **2021**, *12*, 1637–1651.
41. Kolakowski, J.; Djaja-Josko, V.; Kolakowski, M.; Broczek, K. UWB/BLE tracking system for elderly people monitoring. *Sensors* **2020**, *20*, 1574. [CrossRef]

42. Cheong, P.; Rabbachin, A.; Montillet, J.P.; Yu, K.; Oppermann, I. Synchronization, TOA and position estimation for low-complexity LDR UWB devices. In Proceedings of the 2005 IEEE International Conference on Ultra-Wideband, Zurich, Switzerland, 5–8 September 2005; pp. 480–484.
43. Hu, Q.; Yang, J.; Qin, P.; Fong, S.; Guo, J. Could or could not of Grid-Loc: Grid BLE structure for indoor localisation system using machine learning. *Serv. Oriented Comput. Appl.* **2020**, *14*, 161–174. [CrossRef]
44. Bahl, P.; Padmanabhan, V.N. RADAR: An in-building RF-based user location and tracking system. In Proceedings of the Proceedings IEEE INFOCOM 2000. Conference on Computer Communications. NINETEENTH Annual Joint Conference of the IEEE Computer and Communications Societies (Cat. No. 00CH37064), Tel Aviv, Israel , 26–30 March 2000; Volume 2, pp. 775–784.
45. Yeung, W.M.; Zhou, J.; Ng, J.K. Enhanced fingerprint-based location estimation system in wireless LAN environment. In *Emerging Directions in Embedded and Ubiquitous Computing, Proceedings of the EUC 2007 Workshops: TRUST, WSOC, NCUS, UUWSN, USN, ESO, and SECUBIQ, Taipei, Taiwan, 17–20 December 2007*; Springer: Berlin/Heidelberg, Germany , 2007; pp. 273–284.
46. Li, B. Indoor positioning techniques based on wireless LAN. In Proceedings of the 1st IEEE International Conference on Wireless Broadband & Ultra Wideband Communications,Budapest, Hungary, 10–15 July 2005.
47. Saha, S.; Chaudhuri, K.; Sanghi, D.; Bhagwat, P. Location determination of a mobile device using IEEE 802.11 b access point signals. In Proceedings of the 2003 IEEE Wireless Communications and Networking, 2003. WCNC 2003, New Orleans, LA, USA, 16-20 March 2003; Volume 3, pp. 1987–1992.
48. Honkavirta, V.; Perala, T.; Ali-Loytty, S.; Piche, R. A comparative survey of WLAN location fingerprinting methods. In Proceedings of the 2009 6th Workshop on Positioning, Navigation and Communication, Hannover, Germany, 19 March 2009; pp. 243–251. [CrossRef]
49. Yousaf, J.; Zia, H.; Alhalabi, M.; Yaghi, M.; Basmaji, T.; Shehhi, E.A.; Gad, A.; Alkhedher, M.; Ghazal, M. Drone and Controller Detection and Localization: Trends and Challenges. *Appl. Sci.* **2022**, *12*, 12612. [CrossRef]
50. Xu, L.; Yao, S.; Rao, S.; Hu, Q.; Liu, C.; Zhu, H. Indoor Positioning Based on Enhanced 5G Fingerprint Positioning Algorithm. In *Signal and Information Processing, Networking and Computers, Proceedings of the International Conference on Signal and Information Processing, Networking and Computers*; Springer: Berlin/Heidelberg, Germany, 2022; pp. 1179–1184.
51. Ruan, Y.; Chen, L.; Zhou, X.; Liu, Z.; Liu, X.; Guo, G.; Chen, R. iPos-5G: Indoor positioning via commercial 5G NR CSI. *IEEE Internet Things J.* **2022**, *10*, 8718–8733. [CrossRef]
52. Gao, X.; He, D.; Wang, P.; Zhou, Z.; Xiao, Z.; Arai, S. One-Reflection Path Assisted Fingerprint Localization Method with Single Base Station under 6G Indoor Environment. In Proceedings of the 2023 IEEE International Symposium on Circuits and Systems (ISCAS), Monterey, CA, USA, 21–25 May 2023; pp. 1–5.
53. Rathnayake, R.; Maduranga, M.W.P.; Tilwari, V.; Dissanayake, M.B. RSSI and Machine Learning-Based Indoor Localization Systems for Smart Cities. *Eng* **2023**, *4*, 1468–1494. [CrossRef]
54. Liu, W.; Chen, J. UAV-aided Radio Map Construction Exploiting Environment Semantics. *IEEE Trans. Wirel. Commun.* **2023**, *22*, 6341–6355 . [CrossRef]
55. Yang, L.; Chen, H.; Cui, Q.; Fu, X.; Zhang, Y. Probabilistic-KNN: A novel algorithm for passive indoor-localization scenario. In Proceedings of the 2015 IEEE 81st Vehicular Technology Conference (VTC Spring), Glasgow, UK, 11–14 May 2015 ; pp. 1–5.
56. Kemppi, P.; Nousiainen, S. Database correlation method for multi-system positioning. In Proceedings of the 2006 IEEE 63rd Vehicular Technology Conference, Melbourne, VIC, Australia , 7–10 May 2006; Volume 2, pp. 866–870.
57. Nuno-Barrau, G.; Páez-Borrallo, J.M. A new location estimation system for wireless networks based on linear discriminant functions and hidden Markov models. *EURASIP J. Adv. Signal Process.* **2006**, *2006*, 1–17. [CrossRef]
58. Wu, Q.; Liu, H.; Zhang, C.; Fan, Q.; Li, Z.; Wang, K. Trajectory protection schemes based on a gravity mobility model in IoT. *Electronics* **2019**, *8*, 148. [CrossRef]
59. Deng, L.; Yu, D. Deep learning: Methods and applications. *Found. Trends® Signal Process.* **2014**, *7*, 197–387. [CrossRef]
60. Burghal, D.; Ravi, A.T.; Rao, V.; Alghafis, A.A.; Molisch, A.F. A comprehensive survey of machine learning based localization with wireless signals. *arXiv* **2020**, arXiv:2012.11171.
61. LeCun, Y.; Bengio, Y.; Hinton, G. Deep learning. *Nature* **2015**, *521*, 436. [CrossRef]
62. Teo, M.I.; Seow, C.K.; Wen, K. 5G Radar and Wi-Fi Based Machine Learning on Drone Detection and Localization. In Proceedings of the 2021 IEEE 6th International Conference on Computer and Communication Systems (ICCCS), Chengdu, China, 23–26 April 2021; pp. 875–880.
63. Al-Tahmeesschi, A.; Talvitie, J.; López-Benítez, M.; Ruotsalainen, L. Deep Learning-based Fingerprinting for Outdoor UE Positioning Utilising Spatially Correlated RSSs of 5G Networks. In Proceedings of the 2022 International Conference on Localization and GNSS (ICL-GNSS), Tampere, Finland, 7–9 June 2022; pp. 1–7.
64. Njima, W.; Ahriz, I.; Zayani, R.; Terre, M.; Bouallegue, R. Deep CNN for Indoor Localization in IoT-Sensor Systems. *Sensors* **2019**, *19*, 3127. [CrossRef]
65. Yang, S.; Sun, C.; Kim, Y. Indoor 3D localization scheme based on BLE signal fingerprinting and 1D convolutional neural network. *Electronics* **2021**, *10*, 1758. [CrossRef]
66. Walfish, S. A review of statistical outlier methods. *Pharm. Technol.* **2006**, *30*, 82.
67. Fix, E.; Hodges, J.L. Discriminatory analysis. *Nonparametric Discrim. Small Sample Perform. Rep. A* **1951**, *193008*, 238–247.
68. Cover, T.; Hart, P. Nearest neighbor pattern classification. *IEEE Trans. Inf. Theory* **1967**, *13*, 21–27. [CrossRef]
69. Goodfellow, I.; Bengio, Y.; Courville, A. *Deep Learning*; MIT Press: Cambridge, MA, USA; London, UK, 2016.

70. 3GPP. Release 15. 2018. Available online: https://www.3gpp.org/release-15 (accessed on 10 August 2021).
71. 3GPP. Release 16. 2020. Available online: https://www.3gpp.org/release-16 (accessed on 10 August 2021).
72. Open5GS. Open5GS | Open Source Project of 5GC and EPC (Release-16). 2020. Available online: https://open5gs.org/ (accessed on 10 August 2021).
73. Alliance, G.S. OpenAirInterface—5G Software Alliance for Democratising Wireless Innovation. 2020. Available online: https://openairinterface.org/ (accessed on 10 August 2021).
74. free5GC. free5GC 5G Project. 2020. Available online: https://www.free5gc.org/ (accessed on 10 August 2021).
75. Kim, M.; Park, K.; Park, J.; Kim, Y.; Lee, J.; Moon, D. Analysis of Current 5G Open-Source Projects. *Electron. Telecommun. Trends* **2021**, *36*, 83–92.
76. Quectel. 5G RM500Q-GL | Quectel. 2020. Available online: https://www.tekmodul.de/wp-content/uploads/2020/05/Quectel_RM500Q-GL_5G_Specification_V1.0_Preliminary_20200313.pdf (accessed on 3 November 2022).
77. Alliance, W. Wi-Fi CERTIFIED ac | Wi-Fi Alliance—wi-fi.org. Available online: https://www.wi-fi.org/discover-wi-fi/wi-fi-certified-ac (accessed on 7 August 2023).
78. SIG, B. Bluetooth® Core Specification Version 5.0 Feature Enhancements | Bluetooth® Technology Website—bluetooth.com. Available online: https://www.bluetooth.com/bluetooth-resources/bluetooth-5-go-faster-go-further/ (accessed on 8 August 2023).
79. Fractal Networx Limited. TruNET Wireless. 2017. Available online: www.fractalnetworx.com (accessed on 10 July 2023).
80. Raspopoulos, M.; Laoudias, C.; Kanaris, L.; Kokkinis, A.; Panayiotou, C.G.; Stavrou, S. 3D Ray Tracing for device-independent fingerprint-based positioning in WLANs. In Proceedings of the 2012 9th Workshop on Positioning, Navigation and Communication, Dresden, Germany, 15–16 March 2012; pp. 109–113.
81. Jemai, J.; Piesiewicz, R.; Kurner, T. Calibration of an indoor radio propagation prediction model at 2.4 GHz by measurements of the IEEE 802.11 b preamble. In Proceedings of the 2005 IEEE 61st Vehicular Technology Conference, Stockholm, Sweden, 30 May–1 June 2005; Volume 1, pp. 111–115.
82. Upton, G.; Cook, I. *Understanding Statistics*; Oxford University Press: Oxford, UK, 1996.
83. Kingma, D.P.; Ba, J. Adam: A method for stochastic optimization. *arXiv* **2014**, arXiv:1412.6980.
84. Bholowalia, P.; Kumar, A. EBK-means: A clustering technique based on elbow method and k-means in WSN. *Int. J. Comput. Appl.* **2014**, *105*, 17–24. [CrossRef]
85. Kanaris, L.; Kokkinis, A.; Fortino, G.; Liotta, A.; Stavrou, S. Sample Size Determination Algorithm for fingerprint-based indoor localization systems. *Comput. Netw.* **2016**, *101*, 169–177. [CrossRef]